Romanian Reports in Physics **71**, 404 (2019)

ELECTRON TEMPERATURE DETERMINATION OF BISMUTH CONTAINING ELECTRODELESS LIGHT SOURCES DURING SELF-MODULATION REGIME

M. ZINGE[1], Z. GAVARE[1,2], E. BOGANS[1], A. SKUDRA[1], A. FRIDMANE[1]

[1] Institute of Atomic Physics and Spectroscopy, University of Latvia, LV-1050, Skunu Str. 4, Riga, Latvia
[2] Latvia University of Agriculture, Department of Physics, Faculty of Information Technologies, Liela Str. 2, Jelgava, LV-3001, Latvia
E-mail: madara.zinge@gmail.com

Received July 14, 2017

Abstract. In this work we estimate electron temperature in bismuth containing light sources in self-modulation regime. The electron-impact excitation rate coefficients were used in modified Arrhenius form. For the electron temperature determination semilogarithmic plot method together with intensity distribution of Ar spectral lines were used. The experiment results showed that electron temperature in high frequency electrodeless plasma values were around 0.4 eV in maximum phase and 0.6–0.7 eV in minimum phase of the self-modulation regime.

Key words: plasma diagnostics, electron temperature, self-modulation.

1. INTRODUCTION

High-frequency electrodeless lamps (HFEDLs) are widely used as high intensity sources of narrow spectral lines. These lamps have many usages in various optical scientific investigation methods as atomic absorption spectrometry [1], atomic fluorescence spectrometry, and others.

To optimize the light source for particular use it is necessary to understand processes inside the lamp, for instance, interaction between plasma and bulb wall material [2, 3], lamp inner surface changes depending on treatment [4], as well as the processes in discharge plasma and how they influence the emission characteristics of the lamp (for example, intensity, stability and spectral line shapes). Different parameters can give insight into these processes, for example, the gas temperature and electron temperature.

Taking into account that HFEDLs bulbs are sealed vessels it is of particular interest to use non-invasive methods for determination of plasma parameters. For instance, to estimate gas temperature in different kinds of plasmas it is common to use emission of OH [5–7], and other complexes like N_2^+ [8] or C_2 [9].

During our investigations for some HFEDLs besides the stable regime at higher voltage values we have also observed self-modulation – the regime during which the intensity of emission from the lamp changes periodically. In this work we study the changes of electron temperature and spectral line intensities during this regime. Although self-modulation regime can be observed in HFEDLs with different fillings, for instance, with Thallium [10], in this study we will restrict to Bismuth containing HFEDLs.

2. DETERMINATION OF ELECTRON TEMPERATURE

In literature one may find different approaches to determining the electron temperature; for instance, line ratio method [11–14] and theoretical solution of collisional radiative model [15], line-to-continuum method [16], modified Boltzmann plot method [17, 18], and probe methods [13, 19].

In this study electron temperature was determined with semilogarithmic plot method using emission spectra of argon atom under following assumptions:

1) electron energy distribution follows Maxwell distribution function;
2) excited levels are mostly populated by collisions between electrons and atoms in the ground state;
3) excited levels are depopulated mainly by spontaneous emission.

Keeping these assumptions in mind, it is possible to write the excited level population-depopulation balance equation [17]:

$$n_1 \cdot n_e \cdot k_{1i} = n_i \cdot \sum_{i>k} A_{ik} \,, \tag{1}$$

where n_1 is number densities of the ground level; n_e is number densities of electrons; n_i is number densities of the excited level i; k_{1i} is electron impact excitation rate coefficient from the ground level to the excited level i. The last term in formula (1) accounts for all possible radiative transitions from the excited level i to the lower energy levels k.

Total emitted line intensity for a homogeneous light source of length l and for optically thin case can be expressed in following way:

$$I = \frac{1}{4\pi} \cdot \frac{hc}{\lambda_{ij}} \cdot A_{ij} n_i \cdot l \,, \tag{2}$$

where λ_{ij} is wavelength of the transition $i \rightarrow j$; c is velocity of the light in vacuum and A_{ij} is transition probability from level i to j. From this formula it is possible to express number density of the excited level n_i.

The electron-impact excitation coefficient k_{kn} for transition from level k to level n can be found from the following relation:

$$k_{kn} = \int_{E_{th}}^{\infty} \sigma(E) \cdot f(E) \cdot \sqrt{\frac{2E}{m}} \mathrm{d}E \,, \tag{3}$$

where $\sigma(E)$ is electron-impact excitation cross section for transition $k \rightarrow n$; E is energy of the electron; E_{th} is threshold energy for the excitation of the level n; m is mass of the electron and f(E) is electron energy distribution function (EEDF). As mentioned before, in this study it was assumed that free electrons obey Maxwell-Boltzmann distribution, meaning that the expression (3) for electron-impact excitation rate coefficient can be rewritten in the following way:

$$k_{kn} = \int_{E_{th}}^{\infty} \sqrt{\frac{8}{\pi m k_B T_e}} \cdot \sigma(E) \cdot E \cdot \exp\left(-\frac{E}{k_B T_e}\right) \mathrm{d}E \,, \tag{4}$$

where k_b is Boltzmann constant and T_{e} is electron temperature.

To use expression (4), one needs information about excitation cross section dependence on energy. For optically allowed transitions it is more convenient to use semi-empirical formula derived by Drawin [17, 20]:

$$k_{kn} = 8.69 \cdot 10^{-8} \cdot f_{kn} \cdot Z_{eff}^{-3} \cdot \frac{u_1^{3/2}}{u_{kn}} \cdot \Psi_1(u_{kn}, \beta_{kn}) \ [\mathrm{cm^3 s^{-1}}], \tag{5}$$

where f_{kn} is transition oscillator strength; Z_{eff} is effective atomic number (for atomic species $Z_{eff} = 1$); $u_{\mathrm{kn}} = |E_{\mathrm{k}} - E_{\mathrm{n}}|/k_{\mathrm{B}}T_{\mathrm{e}}$; $u_1 = Z_{eff}^2 \cdot 13.6/k_{\mathrm{B}}T_{\mathrm{e}}$; T_{e} is electron temperature and k_{B} is Boltzmann constant. The function $\Psi_1(u_{\mathrm{kn}}, \beta_{\mathrm{kn}})$ accounts for the energy dependence of the cross section, and it can be approximated with following expression [17, 20, 21]:

$$\Psi_1(u, \beta) \approx \frac{e^{-u}}{1+u} \cdot \left(\frac{1}{20+u} + \ln\left[1.25\beta \cdot \left(1 + \frac{1}{u} \right) \right] \right), \tag{6}$$

where $\beta \approx 1$.

For each level considered in this work the electron-impact excitation coefficients k_{1i} were calculated either by combining formulas (5) and (6) or by numerical integration of expression (4), and afterwards fitted using function in form of modified Arrhenius equation (similarly as it was done by authors of [22]):

$$k_{1i} = a_i \cdot (k_B T_e)^b \cdot \exp\left(-\frac{E_{1i}}{k_B T_e}\right), \tag{7}$$

where a_i is transition specific coefficient determined from the fit; b is coefficient determined from the fit ($b \approx 0.2$); E_{1i} is energy of the excited level.

Spectroscopic data of the chosen transitions and obtained fitting parameters are given in Table 1. Spectroscopic data was compiled using NIST database [23].

Table 1

Spectroscopic data (wavelength λ_{ij}, energy of the excited level E_i, transition probability A_{ij}) [23] and fitting parameter a_i for the chosen spectral lines of Ar I

E_i [eV]	ΣA_{ik} [s^{-1}]	a_i	λ_{ij} [nm]	A_{ij} [s^{-1}]
13.153	$3.52 \cdot 10^7$	$6.1197 \cdot 10^{-16}$	772.3761	$5.18 \cdot 10^6$
13.172	$3.44 \cdot 10^7$	$7.8629 \cdot 10^{-16}$	763.5106	$2.45 \cdot 10^7$
13.273	$4.02 \cdot 10^7$	$4.9402 \cdot 10^{-16}$	751.4652	$4.02 \cdot 10^7$
13.283	$3.31 \cdot 10^7$	$5.2352 \cdot 10^{-16}$	714.7042	$6.25 \cdot 10^5$
13.3278	$3.52 \cdot 10^7$	$3.3445 \cdot 10^{-16}$	772.4207	$1.17 \cdot 10^7$
			696.5431	$6.39 \cdot 10^5$
			727.2936	$1.83 \cdot 10^6$
13.3022	$3.46 \cdot 10^7$	$6.9284 \cdot 10^{-16}$	706.7218	$3.80 \cdot 10^6$
			738.398	$8.47 \cdot 10^6$
13.4799	$4.47 \cdot 10^7$	$1.1617 \cdot 10^{-15}$	750.3869	$4.45 \cdot 10^7$
14.711	$5.46 \cdot 10^6$	$2.445 \cdot 10^{-17}$	687.1289	$2.78 \cdot 10^6$
14.839	$5.72 \cdot 10^6$	$1.0636 \cdot 10^{-16}$	703.0251	$2.67 \cdot 10^6$
15.022	$5.10 \cdot 10^6$	$2.7175 \cdot 10^{-16}$	720.698	$2.48 \cdot 10^6$

For levels $3p^5(^2P^o_{1/2})6s^2[1/2]^o_1$ (E_i = 15.022 eV) and $3p^5(^2P^o_{3/2})4d^2[1/2]^o_1$ (E_i = 14.711 eV) electron-impact excitation rate coefficients were calculated using formula (5) (values of oscillator strengths were taken from [24]), for all other levels listed in Table 1 the rate coefficients were found by numerical integration of (4) (data of electron-impact cross sections was taken from [25]).

An example for the fit of excitation rate coefficients calculated using formula (5) is shown in Fig. 1 (for level $3p^5(^2P^o_{1/2})6s^2[1/2]^o_1$ with E_i = 15.022 eV).

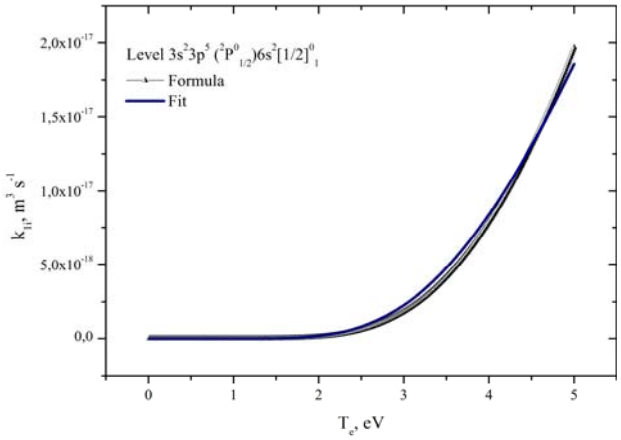

Fig. 1 – Comparison of electron-impact excitation rate coefficient values calculated by formula (5) and fitted with expression (7) for $3p^5(^2P^o_{1/2})6s^2[1/2]^o_1$ excited level of ArI.

An example of the rate coefficient calculated by numerical integration of expression (4) is shown in Fig. 2 (for level $3p^5(^2P^o_{3/2})4p^2[3/2]_1$ with E_i = 13.1531 eV).

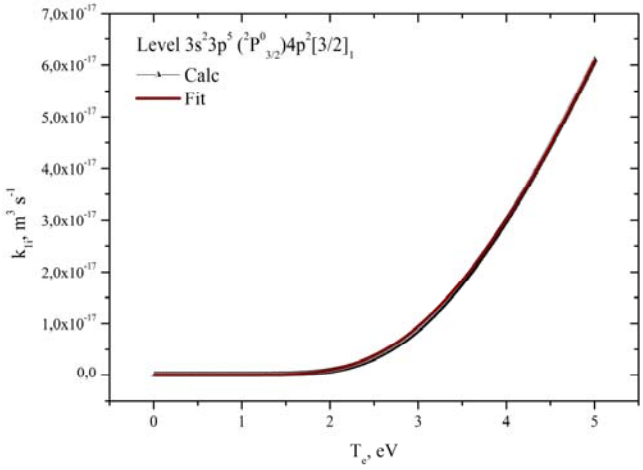

Fig. 2 – Comparison of electron-impact excitation rate coefficient values calculated by numerical integration of expression (4) and fitted with expression (7) for $3p^5(^2P^o_{3/2})4p^2[3/2]_1$ excited level of ArI.

Combining formulas (1), (2) and (7) leads to the following expression:

$$\ln\left(\frac{I\cdot\lambda_{ij}\cdot\sum_{i>k}A_{ik}}{A_{ij}\cdot a_i}\right)=-\frac{E_i}{k_B T_e}+\text{const}. \qquad (8)$$

where “const” combines all the factors which do not depend on the chosen spectral line data.

3. EXPERIMENTAL PART

The light sources under study were HFEDLs filled with bismuth and argon as buffer gas. The lamps were chosen with slightly different fillings: (1) BiI_3 + Ar (p = 400 Pa (3 Torr)) and (2) Bi + SbI_3 + Ar (p = 360 Pa (2,7 Torr)). These lamps are prototypes for use in atomic absorption spectrometers, particularly, Lumex MGA-915M.

The HFEDL vessel is made of glass or quartz and filled with a working element and a buffer gas. These HFEDLs consist of spherical part (with diameter of 1 cm) and small side-arm where excess working element is condensing.

The discharge is ignited at the spherical part of the lamp by placing it into the electromagnetic field of 250 MHz frequency. At first the discharge is observed in the buffer gas, which increases the temperature of the lamp, in turn increasing vapor concentration of the respective element (metal), and the discharge in the vapor ignites.

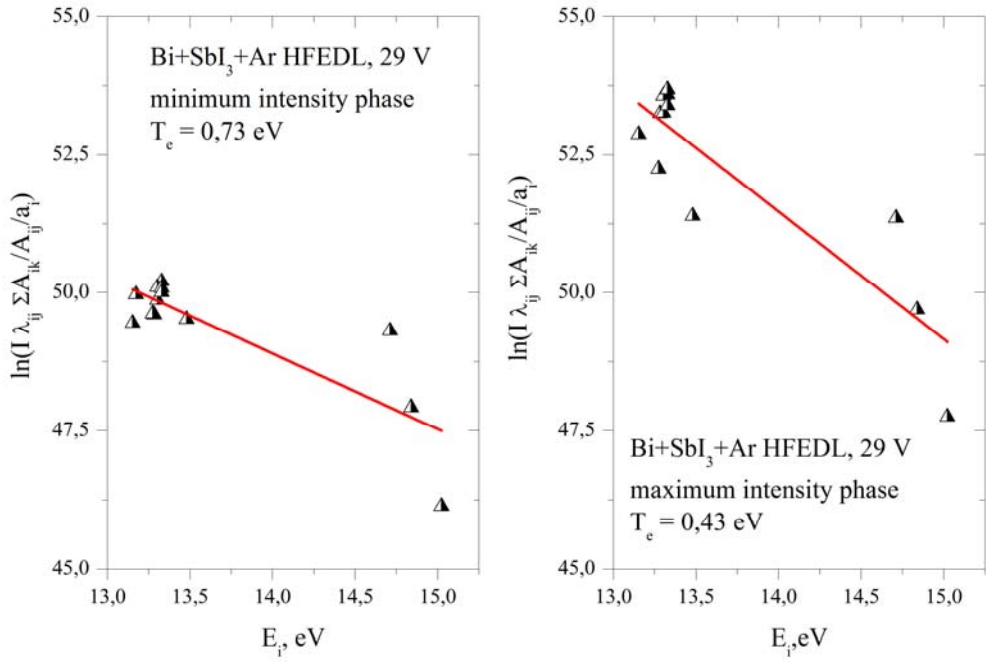

Fig. 3 – Examples of modified Boltzmann plots used to derive electron temperature for $Bi+SbI_3+Ar$ HFEDL during self-modulation regime at: a) maximum intensity and b) minimum intensity. Solid line represents linear fit.

The emission from lamps was registered using JobinYvon SPEX 1000 M spectrometer (focal length 1 m, diffraction grating 1200 mm^{-1}) with charge-coupled device matrix detector (2048 × 512 Thermoelectric Front Illuminated UV Sensitive CCD Detector Simphony). The applied generator voltage values were chosen so that HFEDLs work in self-modulation regime (U = 25 – 29V).

Spectroscopic data from Table 1 together with measured intensities of Ar spectral lines were used to prepare modified Boltzmann plots (in accordance with formula (8)). Electron temperature was then estimated from the slope of the linear fits of these plots. Examples of the obtained modified Boltzmann plots and estimated electron temperatures can be seen in Fig. 3.

4. RESULTS AND DISCUSSION

Each period of the self-modulation regime can be divided into two parts: (1) maximum intensity phase and (2) minimum intensity phase. The measurements were arranged so that each measurement session started with maximum intensity phase.

In emission spectra of both HFEDLs we observed not only atomic spectral lines of Ar and Bi, but BiI vibrational bands (in region around 427 nm), as well.

Figure 4 shows the intensity changes of Bi atomic line and that of BiI (0,0) band head at 427 nm, during the self-modulation regime. In Fig. 4 we can observe the decrease of the BiI (0,0) band head to an intermediate intensity level and immediately after that the sharp decrease of the Bi atomic line. It suggests that BiI complexes play an important role in excitation of atomic species.

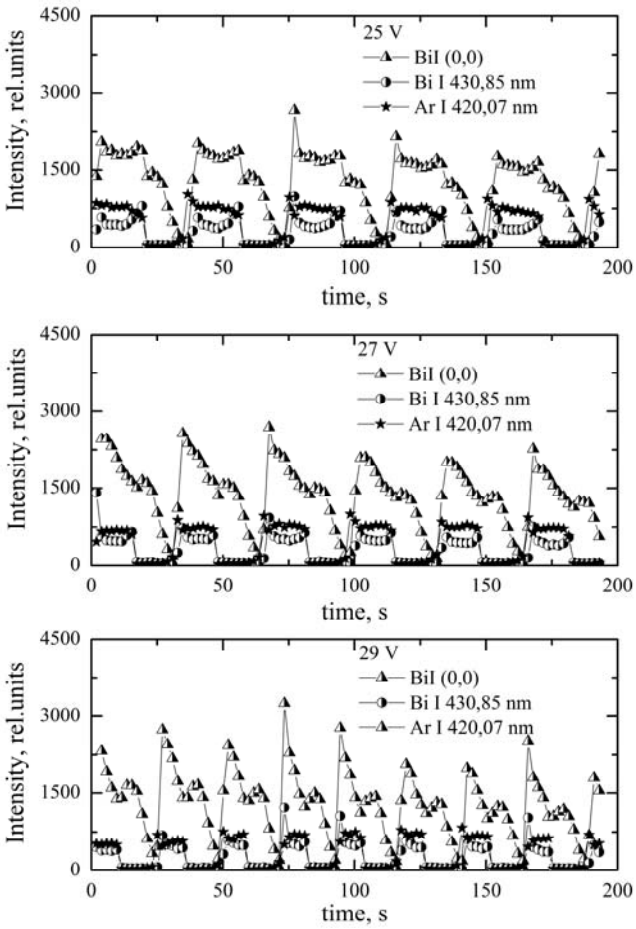

Fig. 4 – Intensity changes of BiI (0,0) band head, Bi I line 430.85 nm and Ar I line 420.07 nm for BiI_3 + Ar HFEDL during self-modulation regime at 25V, 27V and 29V.

The beginning of the maximum phase shows high Ar emission (Bi lines are of lower intensity), during this very small period plasma heats up, it is followed by decrease of Ar intensity because of more efficient excitation of working element of the lamp (in this case, Bi atoms). The maximum phase ends with sharp drop in intensity, which can be explained as follows. With increase in gas temperature the vapor pressure of the working element increases, and electrons more and more

frequently collide with these particles, exciting and ionizing them, until electrons during their free path cannot accumulate enough energy for the excitation and ionization of plasma particles. This in turn leads to decrease of emission intensity. When plasma cools down and electrons are able to get enough energy, the process can start again. This is also indicated by the changes of electron temperature during this regime (Fig. 5).

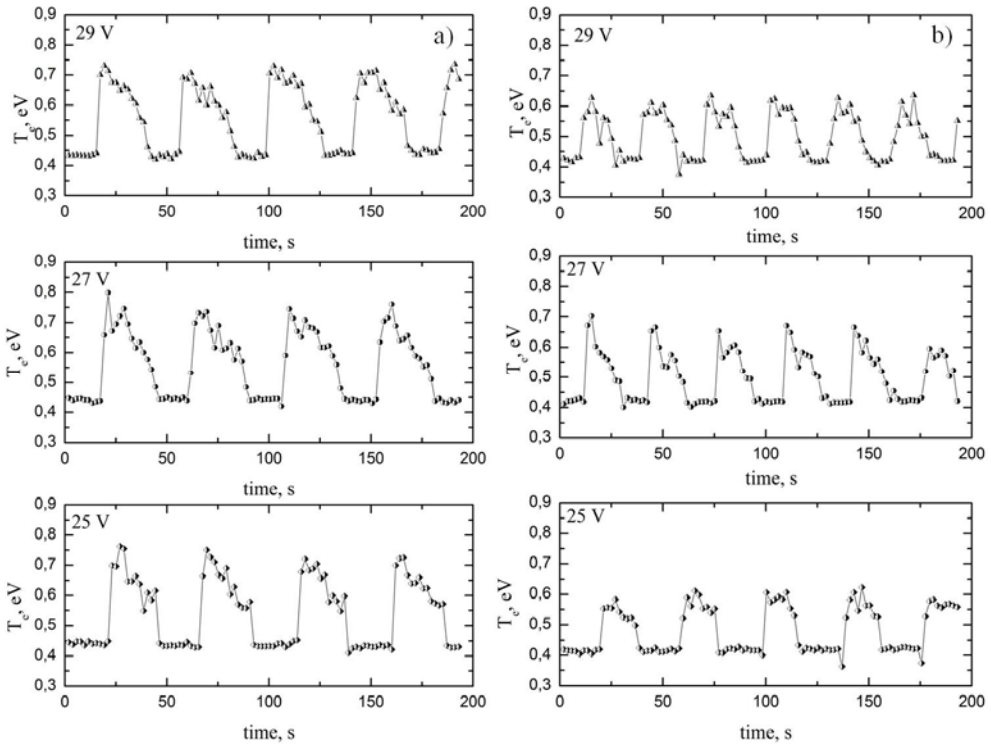

Fig. 5 – Determined electron temperature changes for a) Bi + SbI_3 + Ar and b) BiI_3 + Ar HFEDLs during self-modulation regime at 25 V, 27 V and 29 V.

During the maximum phase for both HFEDLs the determined electron temperature values are around 0.4 eV (slightly higher for Bi + SbI_3 + Ar HFEDL – 0.45 eV), however in minimum intensity for BiI_3 + Ar HFEDL is in range 0.55 – 0.65 eV, but for Bi + SbI_3 + Ar HFEDL electron temperature during this phase is higher, 0.7 – 0.75 eV. For comparison we have also estimated the electron temperature during the stable working regime at lower applied generator voltage. For lamp with antimony the value is higher (above 0.55 eV), but for BiI_3 + Ar lamp the values are in the range 0.4 – 0.45 eV.

Although the determined electron temperature is low (~ 4600–8700 K), it is still higher than the gas temperature (the typical values for HFEDLs are in range

~ 700–1500 K). Authors of [26] have reported that electron temperature of argon ICP is in range 1–2 eV at 13 Pa (100 mTorr) pressure and 6.78 MHz frequency. Results of our experiment are lower which can be explained by the fact that our plasma is excited at higher frequency and the filling is at higher pressure.

Besides the small differences in the values of electron temperature, another difference between the lamps is that of the length of self-modulation period: for antimony containing HFEDL it is longer than for BiI_3 + Ar HFEDL. For both lamps the self-modulation period is under one minute and slightly decreases with increasing the voltage (Fig. 5).

These differences are due to variations in fillings. The antimony, which is added to the one of the lamps, combines with the iodine. It is known that iodine quenches the discharge, so antimony works as stabilizer. It is also the explanation for electron temperature differences during the stable and self-modulation regimes.

5. CONCLUSIONS

In this work we have shown the first results for electron temperature estimation in high-frequency electrodeless lamps containing bismuth. The analysis of the experimental results showed that the estimated electron temperature in Bi containing lamps was around 0.4 eV during maximum intensity phase of the emission and around 0.6–0.7 eV during the minimum intensity phase. The changes in electron temperature agree well with our observations of atomic line intensities during self-modulation regime, as well as with changes of gas temperature during such regime in other lamps [10].

The observed behavior of intensities of Bi atomic lines and BiI band head indicate that these complexes play an important role in excitation of atoms and it should be taken into account.

The experimental results show that addition of antimony to the bismuth containing HFEDL ensures better stability and slightly higher electron temperature values during minimum intensity phase.

Acknowledgments. The work was partially supported by program “Multifunctional materials and composites, photonics and nanotechnology” (IMIS 2, Project No 1, Photonics and materials for photonics).

REFERENCES

1. A. Ganeev et al., Spectrochimica Acta B **58**, 879–889 (2003).
2. A. Skudra et al., Plasma Process. Polym. **4**, S1026–S1029 (2007).
3. A. Skudra et al., Plasma Process. Polym. **6**, S183–S186 (2009).
4. A. Skudra et al., Phys. Stat. Sol. (c) **5**, 915–917 (2008).
5. R. P. Cardoso et al., J. Phys. D: Appl. Phys. **40**, 1394–1400 (2007).

6. C. Engelhard et al., Spectrochim Acta Part B **63**, 619–629 (2008).
7. S. Y. Moon, W. Choe, Spectrochim Acta Part B **58**, 249–257 (2003).
8. G. Gardet, Meas. Sci. Technol. **11**, 333–341 (2000).
9. M. Jimenez et al., International journal of hydrogen energy **38**, 8708–8719 (2013).
10. M. Zinge, Z. Gavare, E. Gosko, Proc. of SPIE **9421**, 94210G, (2014).
11. R. F. Boivin, J. L. Kline, and E. E. Scime, Phys. Plasmas **8**, 5303 (2001).
12. Y Kato et al., Plasma Phys. Control. Fusion **35**, 1513–1528 (1993).
13. A. F. Aleksandrov et al., Plasma Physics Reports **33**, 733–745 (2007).
14. J. B. Boffard et al., J. Phys. D: Appl. Phys. **45**, 045201 (2012).
15. A. Yanguas-Gil, J. Cotrino, and A. R. González-Elipe, Journ. of Appl. Phys. **99**, 033104 (2006).
16. F. Bourg et al., J. Phys. D: Appl. Phys. **35**, 2281–2290 (2002).
17. F. J. Gordillo-Vázquez, M. Camero and C. Gómez-Aleixandre, Plasma Sources Sci. Technol. **15**, 42–51 (2006).
18. Niu Tian-Ye et al., Chinese Phys. **16**, 2757 (2007).
19. Hoyong Park, S. J. You and Wonho Choe, Physics of Plasmas 17, 103501 (2010).
20. H. W. Drawin, F. Klan, and H. Ringler, Zeitschrift fuer Naturforschung **26A**, 186–197 (1971).
21. H. W. Drawin and F. Emard, Physica **85C**, 333–356 (1977).
22. M.J. Schabel, T.W. Peterson and A. J. Muscat, J. Appl. Phys. **93**, 1389–1402 (2003).
23. A. Kramida, Yu. Ralchenko, J. Reader and NIST ASD Team (2015). NIST Atomic Spectra Database (ver. 5.3), [Online].
24. W. F. Chan et al., Phys. Rev. A **46**, 149–171 (1992).
25. A. Yanguas-Gil, J. Cotrino and L. L. Alves, J. Phys. D: Appl. Phys. **38**, 1588–1598 (2005).
26. V. A. Godyak, R. B. Piejak, B. M. Alexandrovich, Plasma Sources Sci. Technol. **11**, 525–543 (2002).